



Effect of deposition temperature and Zn composition on structure, optical and electrical properties of CdO thin films

Sumanth Joishy¹ · B. V. Rajendra¹

Received: 23 March 2018 / Accepted: 26 May 2018 / Published online: 29 May 2018
© Springer Science+Business Media, LLC, part of Springer Nature 2018

Abstract

Cd_{1-x}Zn_xO nanocrystallite films with doping concentrations varied from $x=0.00$ – 0.90 were synthesized through a simple chemical route of the spray pyrolysis process using 0.05M precursor solution. The suitable optimized temperatures for different compositions films were obtained by adjusting deposition temperatures from 693 to 723 K. It was found that structures, surface morphology, optical and electrical properties of the films can be altered by changing Zn contents in CdO deposits. The film composition from $x=0$ to 0.50 have shown cubic phase with (1 1 1) prominent plane and the composition $x=0.90$ shown wurtzite structure with (1 0 1) prominent plane. However, the composition varied from $x=0.60$ to 0.80, in the deposits which showed mixed structure of cubic and wurtzite. The crystallite size, dislocation density and microstrain have been evaluated using XRD data. Scanning electron microscope images have shown different surface morphologies for different Zn doped CdO films. The absorption edge was found to be a blue shift with the increase of Zn content, confirming that there is an increase in the optical band gap. Other optical parameters such as extinction coefficient, Urbach energy, and optical conductivity have estimated using absorption spectra. All films show n-type conductivity, and it decreases with increasing Zn content due to decreasing carrier concentration.

1 Introduction

Nanostructured semiconductors have attracted extensive research attention for the last several years due to their unique properties. The structural, optical and electronic properties of the nanosized structured materials are different in comparison with that of the bulk. Recently extensive work has been reported on transparent conducting oxide (TCO) thin films due to their potential applications in optoelectronic devices, such as light-emitting diodes, laser diodes, solar blind UV detectors, solar cells, photocatalysis, etc. Among several TCO's, cadmium oxide (CdO) has been investigated extensively due to its n-type semiconducting nature, low resistivity and has an optical band gap of approximately 2.5 (eV) [1, 2]. Intentionally variation of composition or introduction of impurities or dopants into a semiconductor is a practical approach to change its electronic structure and then tailoring the electronic and optical properties of the

material [3, 4]. Usually, optoelectronic devices require high transmittance with good conductive films. It is known that it is difficult to obtain a high transmission in the visible region and good conductivity qualities simultaneously.

Zinc oxide (ZnO) is a highly transparent material compared to CdO. Hence, it is expected that the homogeneous composing of these two materials allow intermediate optical and electrical properties between those of pure CdO and ZnO, making it attractive for various applications such as buffer layers on solar cells [5]. ZnO has a wide band gap (3.3 eV at 300 K) and large excitation binding energy (60 meV at 300 K) [6]. The large exciton binding energy of 60 meV of ZnO at room temperature, much larger than those of ZnSe (19 meV), GaN (24 meV) and ZnS (39 meV) is unique to ZnO [7, 8]. The large binding energy facilitates the stable formation of excitons thereby enhancing the efficiency of luminescence and the sensitivity of the photo-response which are an essential requirement for nanoscale optoelectronic devices [9].

The band-gap of CdO thin films can be modified by varying carrier concentration using appropriate growth conditions in addition to composition variation of Zn [10]. For the different applications mentioned before, it is especially important to study the alloy system of the two materials,

✉ B. V. Rajendra
bv.rajendra@manipal.edu

¹ Department of Physics, Manipal Institute of Technology,
Manipal Academy of Higher Education, Manipal 576104,
India

as for how the structure is affected when the composition changes since it is known that ZnO has a hexagonal wurtzite structure and the CdO a cubic one. When CdO is doped with Zn, Zn^{2+} ions can uniformly substitute into the Cd^{2+} sites or interstitial sites in CdO lattice.

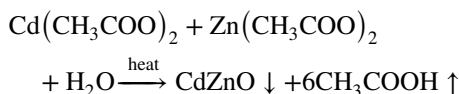
Furthermore, in the case of substitution, a lattice distortion may occur due to their different radii. The relative difference in the melting points of CdO and ZnO may be useful to fabricate CdZnO nanostructure. Further, tuning of the emission from CdZnO in the visible region may make it useful to transparent self-emitting display devices [11]. Since there is phase separation, it is very difficult to attain better quality films. The surface morphology of the film plays a vital role in gas sensor applications. There have been several reports on $Cd_{1-x}Zn_xO$ thin films grown by different deposition methods like spray pyrolysis [12], thermal evaporation [13], molecular beam epitaxy [14], sol-gel [15], sputtering [16] etc. Among these techniques, spray pyrolysis opens up the possibility to control the structure, film morphology and particle size in the nm range. For example, Vigil et al. [17] observed the grains of mixed phase of cubic CdO and hexagonal ZnO for $x \geq 0.40$ for deposited $(ZnO)_x(CdO)_{1-x}$ films by spray pyrolysis. The ZnO crystallites have lower structural perfection than the CdO cubic phase. The optical band-gap varied from 2.29 to 3.28 eV, with increasing x after annealing. However Gupta et al. [18] observed grain morphology along with fiber nature for higher amount of CdO. Whereas, the films having a lower percentage of CdO have shown the only fiber nature very similar to pure ZnO film. Whereas, Santana et al. [19] found the presence of the CdO cubic phase pattern for low Zn concentrations and a mixing of cubic-CdO and hexagonal-ZnO phases for low Cd concentrations. The crystallinity of all samples has improved only after thermal annealing. Sui et al. [20] deposited $Zn_{1-x}Cd_xO$ films in which films with $x = 50\%$ have shown mixed phases of cubic and hexagonal. Whereas, other films have shown single crystalline nature with cubic phase for $x > 50\%$ and hexagonal phase for $x < 50\%$. The resistivity of the films has decreased with increasing Cd content in $Zn_{1-x}Cd_xO$ films. So far our knowledge is concerned; there are very few reports available on the deposition temperature and composition variation of Zn in CdO thin films by a spray pyrolysis method using very low precursor concentration solution. Extensive research work will help to understand the influence of substrate temperature and Zn composition in CdO films on structural, optical and electrical properties. Therefore, a systematic study on the influence of deposition temperature and composition of Zn in the CdO films on the structural, optical and electrical properties are required. Hence, this work primarily focuses on the study of the change in the transport properties of single and mixed phases of spray pyrolysed $Cd_{1-x}Zn_xO$ thin films as a function of various compositions of x and deposition temperature.

2 Experimental details

2.1 Preparation of $Cd_{1-x}Zn_xO$ films

$Cd_{1-x}Zn_xO$ ($x = 0.00-0.90$) thin films were deposited on a glass substrate by cost-effective chemical spray pyrolysis method. Zinc acetate-di-hydrate [$Zn(CH_3COO)_2 \cdot 2H_2O$, Sigma Aldrich, > 99% purity] and Cadmium acetate-di-hydrate [$Cd(CH_3COO)_2 \cdot 2H_2O$, Sigma Aldrich, > 99% purity] were dissolved in double distilled water at a precursor concentration of 0.05M. The solution was sprayed at a rate of 2 ml/min on preheated glass substrate held at different optimized temperatures. The substrate temperature was studied according to the composition variation since the vapor pressure of CdO is greater compared to ZnO. The good films were obtained by optimized temperature for films having composition $x = 0, 0.10, 0.20, 0.30, 0.40$ and 0.50 are 693, 698, 703, 708, 713, and 718 K respectively, 723 K for $x \geq 0.60\%$ Zn. The spray nozzle was fixed at a distance of 28 cm from the substrate. The gas pressure was kept at 5 kg (f)/ cm^2 . After each deposition, the samples were kept same temperatures for 30 min and then cooled back naturally to room temperature. The films having a good homogeneity, stoichiometry, uniform, high adherent and pinhole free were obtained by setting an optimized preparation condition (Table 1).

Chemical reaction:



2.2 Characterization of deposited films

The thickness of the films was measured from DektakXT Surface Profile Measuring System (Bruker Model no. DXT-18-1715). Rigaku Miniflex 600, diffractometer with CuK_α radiation (1.5405 Å) over the range $2\theta = 20^\circ-80^\circ$ was used for structural studies. The morphological and compositional studies of the films were carried out by Scanning Electron Microscopy (SEM) (Zeiss EVO 18-15-57) and Energy dispersive X-ray analysis (EDAX). Optical studies were done using Shimadzu-1800 UV-Vis spectrophotometer in the range from 350 to 800 nm in both absorption and transmittance modes. The measurements of electrical resistivity and carrier concentration were recorded using a Keithley 6220 source meter and magnetic field of 0.5 T by Van der Pauw technique. An optical microscope was used to check the uniformity, homogeneity and pin hole free surface of deposited films. The film's adherence was confirmed by mechanical tap technique.

Table 1 Optimized deposition conditions used to deposit $\text{Cd}_{1-x}\text{Zn}_x\text{O}$ films using 0.05 molarity solution

Solute	Cadmium acetate di-hydrate and Zinc acetate di-hydrate						
Solvent	Double distilled water						
Concentration of solution	0.05M						
Composition of (Zn)	$x = 0.00\text{--}0.90$ at. %						
Carrier gas	Compressed air 5 kg(f)/ cm^2						
Solution spray rate	2 ml/min						
Substrate temperatures for various x values	693 K	698 K	703 K	708 K	713 K	718 K	723 K
	0.00	0.10	0.20	0.30	0.40	0.50	0.60–0.90
Substrate to nozzle distance	28 cm						
Film thickness	500–550 nm						

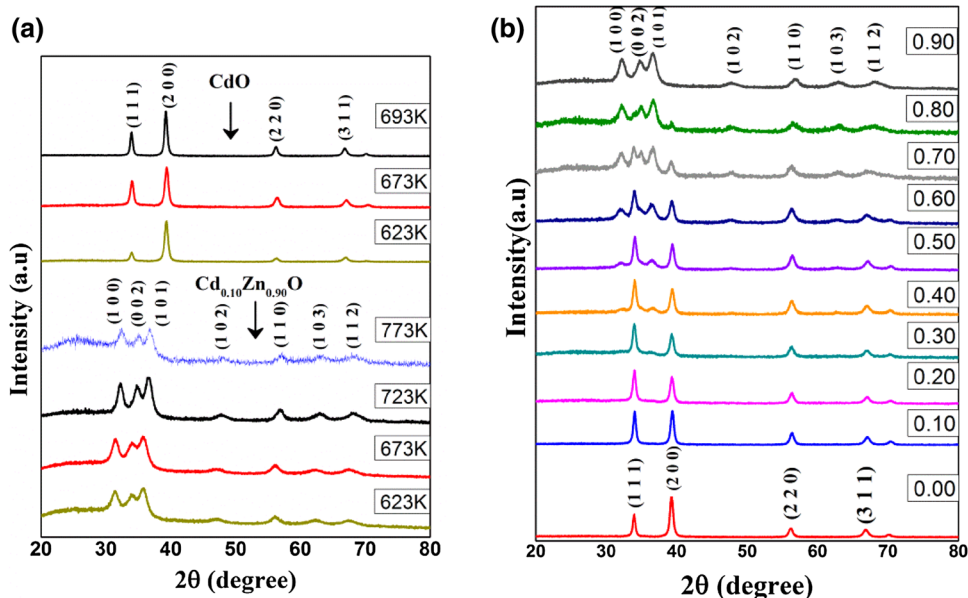
3 Results and discussion

3.1 Structural properties

The XRD patterns of pure CdO and $\text{Cd}_{0.10}\text{Zn}_{0.90}\text{O}$ thin films with different growth temperatures are shown in Fig. 1a. The films have shown cubic and wurtzite structure for CdO and $\text{Cd}_{0.10}\text{Zn}_{0.90}\text{O}$ respectively. The diffraction peak intensity had increased with increasing substrate temperature, indicating the enhancement of crystallinity. On the other hand, at the higher deposition temperature, the premature decomposition of precursor before reaching the substrate might be the reason for the amorphous nature of the film. Similar kind of result was also noticed by Singh et al. [21] for the spray deposited nano-crystalline CuO films. Figure 1b shows the XRD graph of $\text{Cd}_{1-x}\text{Zn}_x\text{O}$ thin films for different Zn dopant. These results demonstrated that the films were grown with a cubic structure and the peaks were assigned to (1 1 1), (2 0 0), (2 2 0) and (3 1

1) plane for x up to 0.50. With increasing x value above 0.50, the transition from the cubic structure to a hexagonal form occurred. In composition $x = 0.50\text{--}0.80$, the mixture of hexagonal and cubic structures with strong peaks along (1 0 1) and (2 0 0) were observed respectively. Whereas for $x = 0.90$ the crystal structure of thin film was hexagonal and all the peaks were assigned to (1 0 0), (0 0 2), (1 0 1), (1 0 2), (1 1 0), (1 0 3) and (1 1 2) diffraction lines of wurtzite $\text{Cd}_{1-x}\text{Zn}_x\text{O}$. The prevalent presence of the crystalline cubic phase for below 50% Zn dopant agrees with the trend observed for other II-IV based mixed thin film oxides [5]. This may be attributed to their same electrovalence and similar Pauling electronegativities (1.65 for Zn and 1.69 for Cd). Incorporation of Zn in CdO lattices results in shifting of a diffraction peak to higher angles since the ionic radius of Zn is slightly lesser than Cd. The mixture of the two structures was observed in the films of dopant intermediate between 20 and 50%. Since for high values of Zn concentration, films grow with small crystalline grains of ZnO. The decrease in peak intensity is attributed due

Fig. 1 a XRD patterns of CdO and $\text{Cd}_{0.10}\text{Zn}_{0.90}\text{O}$ films deposited at different substrate temperatures of 0.05M concentration and b $\text{Cd}_{1-x}\text{Zn}_x\text{O}$ films ($x = 0.0\text{--}0.90$) deposited at optimized temperature



to the effect of Zn content in the lattice of CdO thin films. The decrease in full-width half maxima (FWHM) of diffraction peaks for mixed phase films results in an increase of crystallite size with increasing Zn content.

The mean crystallite size of the films was calculated using the Scherrer's formula [12]

$$D = \frac{0.9\lambda}{\beta \cos \theta} \quad (1)$$

where θ is the Bragg's angle, λ is the wavelength of X-ray and β is the FWHM.

The other microstructural parameters such as microstrain (ϵ), dislocation density (δ) and the number of crystallites per unit area (N) of the films were calculated using following equations [22, 23].

$$\epsilon = \frac{\beta \cos \theta}{4} \quad (2)$$

$$\delta = \frac{n}{D^2} \quad (3)$$

$$N = \frac{t}{D^3} \quad (4)$$

where n is a factor which equals unity giving a minimum dislocation density, t is the thickness of the thin films.

The average crystallite size is found to increase slightly with increase in the substrate temperature. This can be attributed to the improvement of crystal quality due to the periodic arrangements of atoms in the crystal lattice. The increase in deposition temperature (reaction temperature) results in grain growth, thereby an increase in crystallite size. A slight change in dislocation density, strain and number

of crystallites per unit area with deposition temperature are presented in Fig. 2a. The smallest value of dislocation density and strain for optimized temperature indicates minimum defects compared with the films deposited for other substrate temperatures. The crystallite size was calculated using prominent peaks of all deposited films. Figure 2b, it is found that least crystallite size was 9 nm for $x = 0.70$ at.% Zn content. Variation of crystallite size with Zn composition is probably indicating that incorporation of Zn in CdO is contributing to the change in crystallinity as well as the preferred growth orientation of CdO thin films. The presence of dislocation density and micro-strain strongly influences many of the properties of materials. Hence the determination of these quantities is essential to study the structural properties of the deposits. The micro-strain in the films is slightly increased with respect to Zn doping concentrations. In addition, since the ionic radius of Zn^{2+} ions is slightly lesser than Cd^{2+} ions, the strain in CdO lattice is influenced by Zn^{2+} and thereby alters the preferential growth. Zinc incorporation will lead to the lattice contraction and will cause the appearance of the tensile stresses. It is due to the difference in ionic radii between zinc and cadmium [24].

The lattice parameters 'a' and 'c' for hexagonal structure can be calculated from below relation

$$\frac{1}{d^2} = \frac{4h^2 + hk + l^2}{3a^2} + \frac{l^2}{c^2} \quad (5)$$

The lattice parameter 'a' for cubic structure can be calculated from relation given below

$$d = \frac{a}{\sqrt{(h^2 + k^2 + l^2)}} \quad (6)$$

The variation in the lattice parameter is listed in Table 2.

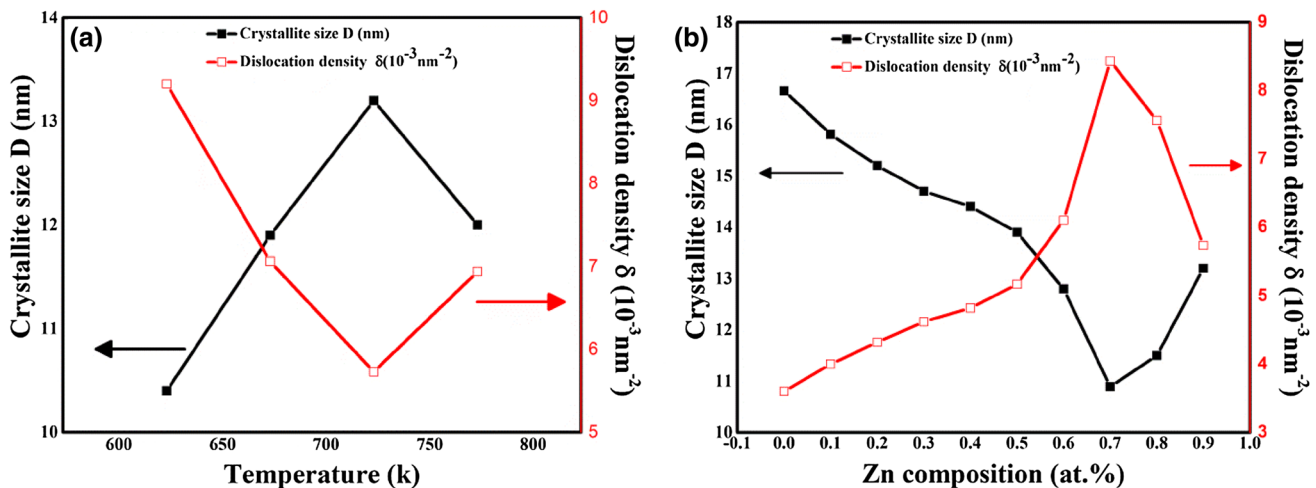


Fig. 2 Crystallite size and dislocation density versus **a** substrate temperature and **b** Zn concentration in $\text{Cd}_{1-x}\text{Zn}_x\text{O}$ films

Table 2 Evaluated lattice parameters, number of crystallites per unit area and micro strain of Cd_{1-x}Zn_xO films prepared using 0.05M solution molarity

Samples	Deposition temperature (K)	Lattice constant (Å)		Number of crystallites per unit area 'N' ($\times 10^{16} \text{ cm}^{-2}$)	Strain ϵ ($\text{lines}^{-2} \text{ m}^{-4}$)
		Hexagonal	Cubic		
CdO	623		a=4.590	12	0.091
	673		a=4.595	11	0.086
	693		a=4.597	11	0.084
Cd _{0.90} Zn _{0.10} O	698		a=4.594	13	0.079
Cd _{0.80} Zn _{0.20} O	703		a=4.591	15	0.114
Cd _{0.70} Zn _{0.30} O	708		a=4.589	17	0.119
Cd _{0.60} Zn _{0.40} O	713		a=4.586	18	0.203
Cd _{0.50} Zn _{0.50} O	718	a=3.245 c=5.239	a=4.588	20	0.089
Cd _{0.40} Zn _{0.60} O	723	a=3.230 c=5.235	a=4.591	26	0.110
Cd _{0.30} Zn _{0.70} O	723	a=3.226 c=5.223	a=4.589	42	0.142
Cd _{0.20} Zn _{0.80} O	723	a=3.217 c=5.200	a=4.587	36	0.152
Cd _{0.10} Zn _{0.90} O	623	a=3.2608 c=5.2802		48	0.160
	673	a=3.2007 c=5.1366		32	0.156
	723	a=3.3007 c=5.3062		23	0.141
	773	a=3.1886 c=5.1036		31	0.150

A slight variation in lattice parameter *c* upon Zn doping was observed, which indicates that the samples were in a uniform state of stress with tensile component parallel to *c*-axis [24]. The other possible reason for the variation might be because of the variation in the linear thermal expansion coefficients of CdZnO film and glass.

3.2 Surface morphology

During the pyrolytic decomposition of the sprayed droplets onto the hot substrates, different atomic rearrangement processes are responsible for the different surface topographies of the thin films. The improvement of the crystal structure, as well as the homogeneity and well distribution of grains that are coalesced in the form of nanoclusters with increasing substrate temperature, were observed. Since the increase in temperature has provided enough energy for nucleation. At lowest substrate temperature, the film was dense, and grains were unclear. For films deposited at a higher temperature, the grain boundaries can be distinguished clearly. It is clear that the grain size increased with increasing substrate temperature. With Zn doping the films become relatively more compact and uniform with tiny crystallites. The grain growth due to the agglomeration, coalescence and aggregation events during

the deposition causes the improvement. The agglomerations of grains to form smaller particles are noticeable in all the films (Fig. 3). The films having mixed phase leads to the formation of a dense surface with irregularly shaped agglomerations of grains. The grains are larger and show smooth, regular arrangement. For all the films rather a rough surface was observed. The films of less Zn content are slightly different in comparison to others. The grains are better resolved and can be identified more clearly. This correlates with XRD results, which revealed that the films with less Zn content characterized by smallest value of the strain and smallest zinc content in comparison to other films. The uniform distribution of fibrous structure was observed for the deposits having 90% of Zn content. The fibrous structure occurs may be due to during the drying process, compressive membrane force is generated. This leads to twisting of the gelated thin films and creates disordered wrinkles in the form of fibers. It should be noted that the developed surface texture is required to provide light scattering and subsequent light trapping inside the silicon solar cell structure. The doping concentration has a regular effect on the grain structure. Which is contradictory with the results of Khranovsky et al. [25] in which they have not seen any obvious effect on the grain structure in film morphology. The obtained structures play great

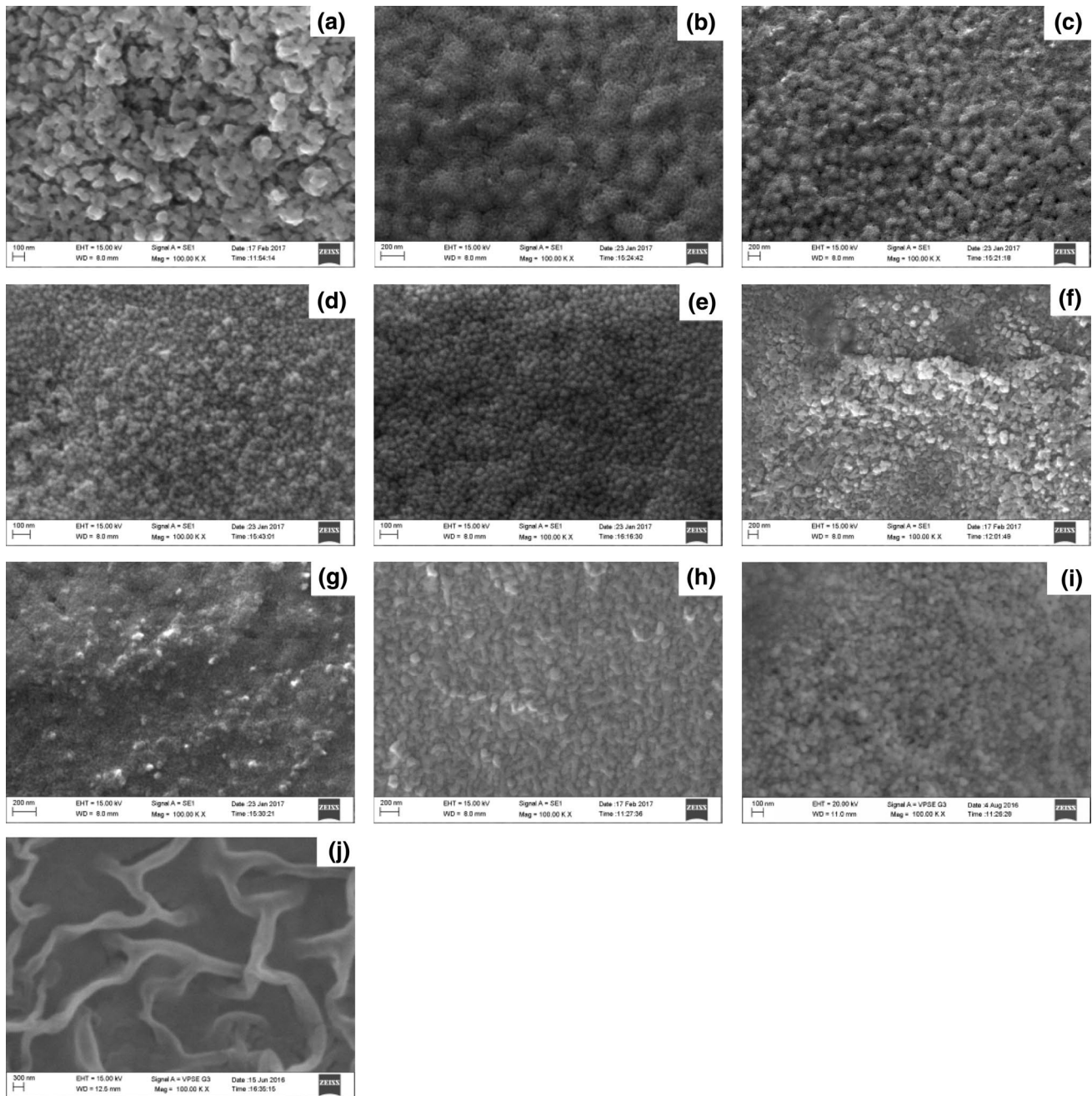


Fig. 3 a–j SEM images of $\text{Cd}_{1-x}\text{Zn}_x\text{O}$ films for different values of x from 0.00 to 0.90

role in device applications such as solar cells, gas sensors due to their high specific surface area and adsorption capacity. The obtained fibrous and spherical grain nature of the surface could be considered good for the chemical reaction and diffusion process needed for the sensing mechanism. The simplicity of fabrication of nanostructured CdZnO facilitates tailoring its surface with higher surface area. This will help to boost adsorption of various gases for their effective detections. Moreover, due to the fibrous structure of 90% Zn doped film, which offers high

surface-to-volume ratio, it leads to increase in the number of adsorption sites for gaseous molecule interaction with the surface.

Table 3 Compositional and elemental analysis done by EDAX spectrum

Element	Atomic %
Zn K	80.88
Cd L	19.12
Totals	100.00

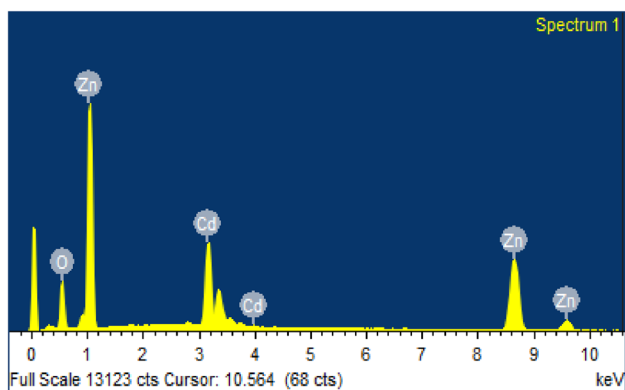


Fig. 4 Typical EDS spectrum recorded for $\text{Cd}_{0.20}\text{Zn}_{0.80}\text{O}$ films

Table 3 summarizes the compositional and elemental analysis done by energy dispersive analysis of X-rays (EDAX) spectrum (Fig. 4). Three peaks related to Zinc, Oxygen, and Cadmium were identified. This confirms the incorporation of Zn content into the CdO films using spray pyrolysis. The smoothness of the films stayed unaltered even after the addition of Zn in CdO, which is generally found in the doping process. Other elements like Si, Ca and O were present due to glass substrates. These elements were eliminated in the EDAX spectrum used for compositional analysis. The ratio of Cd and Zn cations becomes important for obtaining a TCO film.

3.3 Optical properties

The transmittance of the samples was measured as a function of the wavelength in the range of 300–800 nm. Figure 5a for all prepared films indicates, there is a small and

gradual increase in the optical transparency in the visible region, and some saturation occurs in the infrared region that reaches to more than 90% with a relative change in the absorption edge. An increase in the transparency with an increase in the substrate temperature was observed which may be due to the improvement of the film crystal structure. The blue shift can be explained by one of the mechanisms of the Burstein–Moss effect [26], which was from the Fermi level motion leading to an increase in the charge carrier concentration when the temperature of the thin films increased. The incomplete decomposition of the precursor, which leads to exist residual organic components in the films, and low crystal quality of films at low temperatures create defects which result in strongly absorbed visible light. The films deposited at high temperature were highly transparent in the visible region, but their UV transmission was low. The substrate temperature provides enough energy for nucleation, and it shows better crystal quality for higher temperature. The films deposited at 773 K shown decrease of transmittance due to the diminished quality of deposits created by defects at higher temperature. This may also be due to the limitation of the transition temperature of borosilicate glass substrate (above 723 K). In this context, we identified optimized substrate temperatures for different Zn composition among the many different trials, as it provided the required thermal energy for proper decomposition of the precursor salt and the crystallization of $\text{Cd}_{1-x}\text{Zn}_x\text{O}$ thin films, which has been mentioned in Table 2.

Figure 5b shows the optical transmittance of $\text{Cd}_{1-x}\text{Zn}_x\text{O}$ films where transmittance increases with Zn content in the deposited films. The high transparency is associated with a good structural homogeneity. The $\text{Cd}_{1-x}\text{Zn}_x\text{O}$ film with high Cd content will induce more crystalline defects like

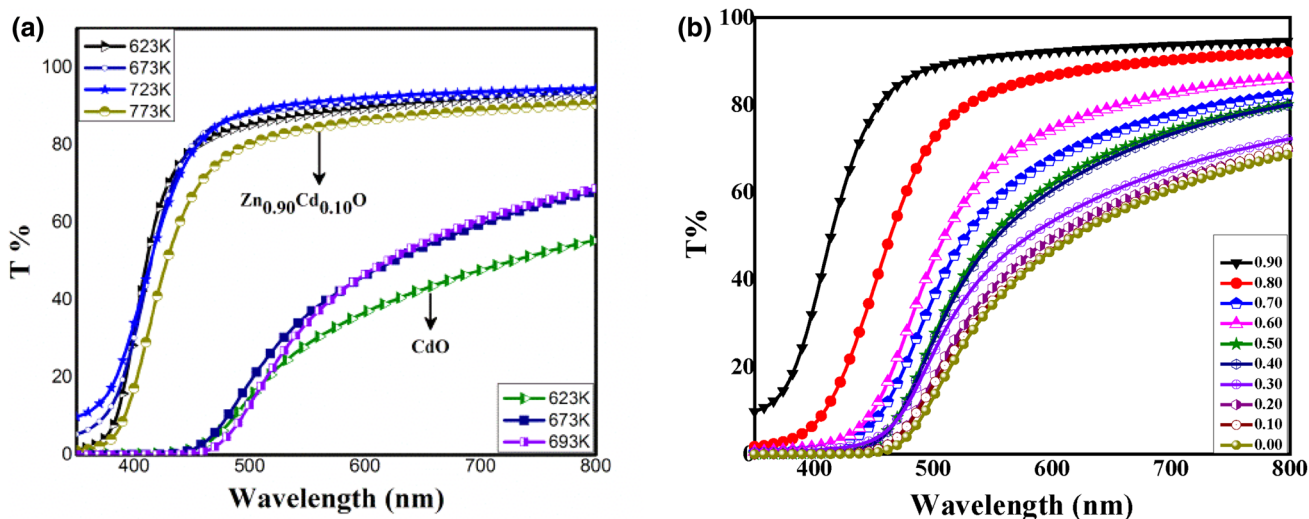


Fig. 5 Optical transmission spectrum of **a** pure CdO and $\text{Cd}_{0.10}\text{Zn}_{0.90}\text{O}$ films deposited at different substrate temperatures and **b** $\text{Cd}_{1-x}\text{Zn}_x\text{O}$ films with different composition using 0.05M solution molarity

oxygen vacancies, cadmium and zinc interstices which as scattering centers would reduce the optical transmittance [27]. These decreases in the transmittance values in the CdO films having less amount of Zn content may be due to the grain boundary scattering. It is also due to the absorption of the visible light by Cd nanoparticles. In transparent metal oxides, the metal to oxygen ratio and crystal orientation decides the transmittance. A metal-rich film usually exhibits less transparency [28]. The increase of transmittance with Zn dopant films could be applicable for window layer in solar cells.

The optical energy band gap of the film was estimated from the fundamental absorption edge of the films. The relation between the absorption coefficient (α) and photon energy ($h\nu$) optical transition is given as,

$$(\alpha h\nu) = A(h\nu - E_g)^n \quad (7)$$

where ' α ' is the absorption coefficient, A is an energy-independent constant and E_g is the optical energy band gap and the value $n = 1/2$ or 2, for direct and indirect allowed transitions respectively.

Figure 6a and b shows the variation of $(\alpha h\nu)^2$ versus $h\nu$ for different substrate temperatures and Zn content level in $Cd_{1-x}Zn_xO$ films respectively. The energy band gap was determined by extrapolating the linear portion of the plot $(\alpha h\nu)^2$ versus $h\nu$ to the energy axis at $\alpha = 0$. It was observed that the optical band gap values increased with increasing temperature, which can be due to improvement in crystallinity of the samples as supported by XRD studies. It can also be observed that the optical band gap increases from 2.18 to 3.03 eV with increasing Zn concentrations, which is in good agreement with the previous reports [29]. As the band gap of ZnO is larger than CdO, while alloying of Zn, the 5s electron state of Cd, below the conduction band will become less predominant than the high energy 4s state of Zn. This shifts the conduction band edge upwards and results in an increase in the band gap [30]. Hence, the absorbance below 465 nm makes Cd_{0.10}Zn_{0.90} film a righteous choice of light detectors from UV to blue region. It

is noticed that the band gap of CdO is initially increased from 2.18 to 2.54 eV up to 0.60 at% Zn doping, and then slightly decreased to 2.46 eV for 0.70 at% Zn doping and for higher doping concentration, band gap again increased with increase in Zn doping concentration (Fig. 6c). The trend of energy band gap variation is correlated with the crystallite size, which was decreased with increasing Zn dopant due to the ionic radius of Zn is smaller than Cd. Up to 0.6% of Zn, the prominent peak was related to Cd. Thereafter, it was suddenly changed to Zn and crystallite size was found to increase. At 0.7% Zn doping there was a complete change in film properties confirmed by XRD. Tang et al. [31] applied the first-principles calculation to study wurtzite $Zn_{1-x}Cd_xO$ alloys with different Cd dopant. They attributed the reduction of band gap with the increase of Cd content to the contributions of the hybridization of electronic states of Zn-4s and Cd-5s, the enhancement of p-d repulsion and the tensile strain due to Cd-doping. The tailoring of the optical band gap should help in designing a particular Zn: CdO film for its use in solar energy storage devices. For solar cell applications, TCO's should have widened the band gap and the widened band gap values obtained here for CdZnO films make them suitable for photovoltaic solar cells and other optoelectronic devices.

Urbach energy and extinction coefficient of the films have strongly dependence on the deposition temperature and Zn doping concentration. The absorption coefficient shows exponential energy dependence, referred to the Urbach tail. Urbach energy and extinction coefficient are calculated by the relations [18]:

$$\alpha = \alpha_0 \exp\left(\frac{h\nu}{E_U}\right) \quad (8)$$

$$K = \frac{\alpha \lambda}{4\pi} \quad (9)$$

where α is an absorption co-efficient, λ is the wavelength. E_u is the Urbach energy which corresponds to the width of

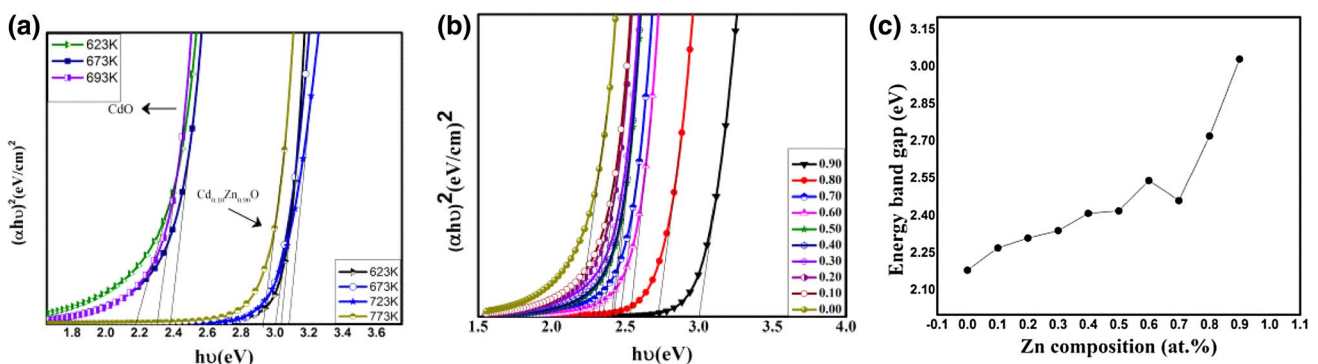


Fig. 6 $(\alpha h\nu)^2$ versus $h\nu$ plot of **a** CdO and Cd_{0.10}Zn_{0.90}O films deposited at different substrate temperatures, **b** Cd_{1-x}Zn_xO films with different x values using 0.05M concentrations and **c** band gap energy as a function of Zn content in the films

the band tail. Thus, a plot of $\ln \alpha$ versus photon energy (eV) should be linear and Urbach energy is calculated from the reciprocal gradient of the linear portion of curves.

The Urbach tail is the width of the localized states available in the optical band gap [32]. Figure 7a and b shows the linear curves of $\ln(\alpha)$ versus photon energy (eV) for different substrate temperature and Zn dopants respectively. The linear behavior obtained between $\ln(\alpha)$ and $h\nu$ in the strong absorption region suggests the transition between the occupied states of the valance band tail to unoccupied states in the conduction band. Decrease of disorder in the band edge with increasing deposition temperature, which varies inversely with values of the energy band gap. The Urbach energy for different temperatures of deposit $\text{Cd}_{0.10}\text{Zn}_{0.90}\text{O}$ and CdO was varied from 0.25 to 0.22 eV and 0.84 to

0.80 eV respectively. The Urbach energy was varied from 0.80 to 0.22 eV for the deposits with different Zn content.

Figure 8a and b depicts the extinction coefficient of the films for different substrate temperature and Zn dopants respectively. It has an inverse relation with the transmittance spectrum. The source k (absorption) refers to the inelastic scattering of the electromagnetic waves in the semiconductor such as the Compton effect, photoelectric effect, pair production effect and so on [33]. The change in extinction coefficient along with the increase in temperature may be attributed to the temperature dependence of the electronic polarizability at constant volume. Meanwhile, it decreases with increasing wavelength. This suggests that the $\text{Cd}_{1-x}\text{Zn}_x\text{O}$ thin film shows a normal dispersion. The (low) high transmittance spectra have (high) low optical constants.

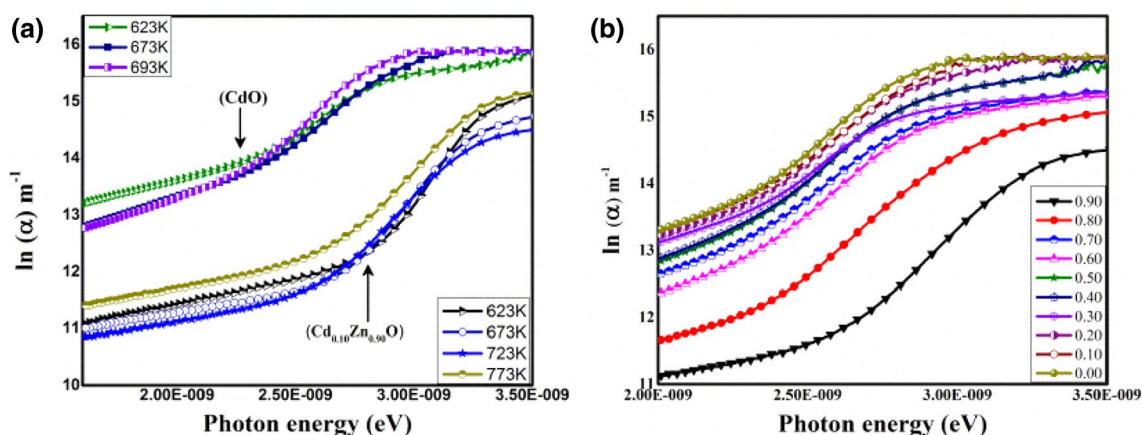


Fig. 7 Variation of $\ln(\alpha)$ versus photon energy of a pure CdO and $\text{Cd}_{0.10}\text{Zn}_{0.90}\text{O}$ films deposited at different substrate temperatures and b $\text{Cd}_{1-x}\text{Zn}_x\text{O}$ films prepared using 0.05M molarity solution

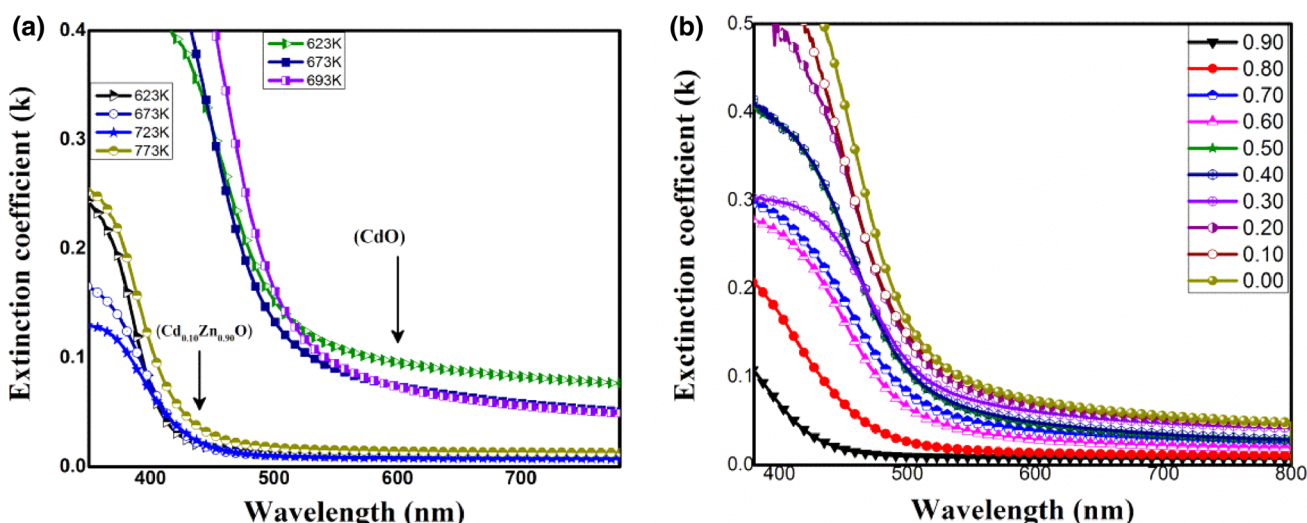


Fig. 8 Variation of extinction co-efficient (K) with wavelength of a pure CdO and $\text{Cd}_{0.10}\text{Zn}_{0.90}\text{O}$ films deposited at different deposition temperatures and b $\text{Cd}_{1-x}\text{Zn}_x\text{O}$ films prepared using 0.05M molarity solution

The low value of extinction coefficient in the visible region, it is a qualitative indication of excellent surface smoothness of the CdZnO thin film.

The optical conductivity (σ) of the films was calculated using the relation [34],

$$\sigma = \frac{\alpha nc}{4\pi} \quad (10)$$

where c is light velocity in a vacuum. The variations of the optical conductivity with incident photon are shown in Fig. 9. The optical conductivity describes the free charges. It is more for high Cd content films and films deposited for high substrate temperature. The gradual modification of optical conductivity of the deposits with substrate temperature was noticed (Fig. 9a). The optical conductivity dramatically changes, which means that available free carriers absorb photon energy and hence maximum optical conductivity is observed in less Zn doped CdO films (Fig. 9b).

3.4 Electrical properties

Hall measurements were performed at room temperature to characterize the electrical properties of $\text{Cd}_{1-x}\text{Zn}_x\text{O}$ films, such as to identify the conductivity type and to determine the resistivity and carrier concentration. All deposits have shown n-type conductivity, which is confirmed by the negative sign of Hall coefficient. The variation in electrical properties such as resistivity (ρ) and carrier concentration (n_e) of Zn doped CdO thin films is as shown in Table 4. The increase in resistivity with high Zn-doped film can be attributed to the deterioration of crystallization quality because the charge carriers will decrease due to the longer carrier path length and the increase in the scattering of the charge carriers at the crystal defects [35]. For mixed

Table 4 Electrical resistivity and carrier concentration of $\text{Cd}_{1-x}\text{Zn}_x\text{O}$ thin films prepared using 0.05M solution molarity

Zn content (at.%)	Resistivity ρ (Ω cm)	Carrier concentration n (cm^{-3})
0.00	0.00002	1.31×10^{22}
0.10	0.00008	3.78×10^{22}
0.20	0.00052	1.11×10^{21}
0.30	0.0012	1.42×10^{20}
0.40	0.007	1.08×10^{19}
0.50	0.068	7.99×10^{18}
0.60	1.378	4.47×10^{17}
0.70	1.212	6.73×10^{17}
0.80	3.021	8.91×10^{16}
0.90	4.042	7×10^{16}

phase films, the cadmium atoms may also segregate at the grain boundaries in the form of amorphous cadmium components, which will increase the grain boundary barrier. Thus, the mobility of charge carrier decreases as more scattering and grain boundary barrier effects occur. This might be the reason for high values of resistivity. The carrier concentration of CdO thin films was decreased with the increasing Zn concentration. The large value of the carrier concentration in low Zn content films may be due to the interstitial occupation of some Cd^{2+} ions, which donates two electrons to the conduction band. For mixed phase of films, less carrier concentration was observed. This may be because of increased lattice distortion.

Enhancement of the migration of smaller crystallites and joining of similarly oriented grains reduces the scattering of electrons, which increases the mobility of charge carriers. Improvement in electrical properties for less Zn doped CdO

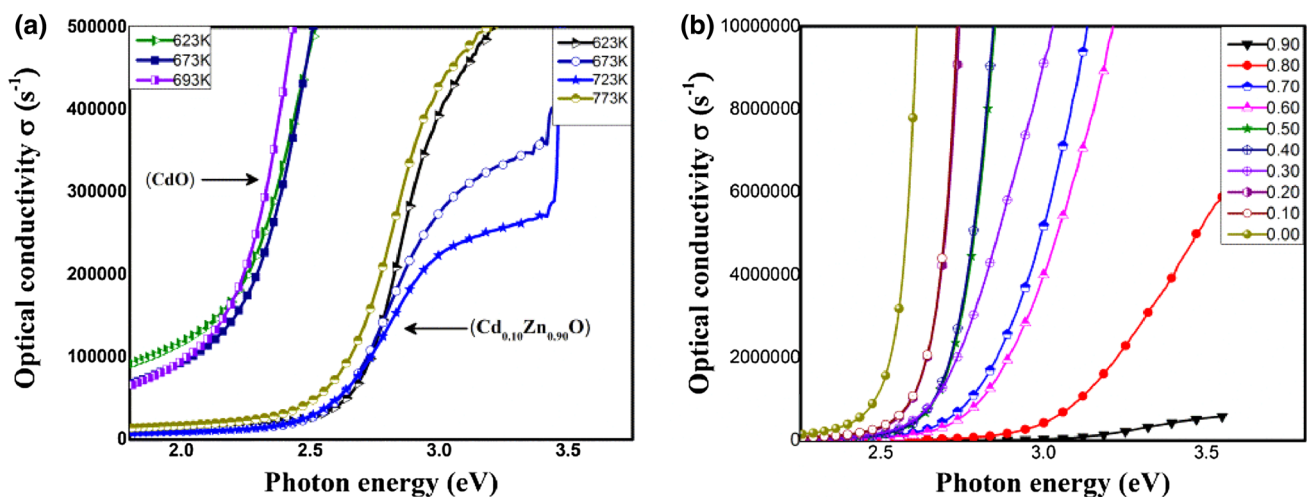


Fig. 9 Optical conductivity of the films versus incident photon $h\nu$ of **a** pure CdO and $\text{Cd}_{0.10}\text{Zn}_{0.90}\text{O}$ films deposited at different substrate temperatures and **b** $\text{Cd}_{1-x}\text{Zn}_x\text{O}$ films deposited using 0.05M molarity solution

Table 5 Comparison of Zn_{0.50}Cd_{0.50}O film result with previous reports

Reports	Structure	Crystallite size (nm)	Surface morphology	Energy band gap (eV)	Resistivity ρ (Ω cm)	References
Sumanth	Mixed phase	13.2	Spherical nano grains	2.41	0.068	
Vigil et al.	Amorphous			2.59	0.06	[17]
Gupta et al.			Fibrous	2.49		[18]
Santana et al.	Amorphous			2.60		[19]
Sui et al.	Mixed phase			2.92, 2.31	0.01	[20]
Tabet et al.	Amorphous			2.35		[29]
Caglar et al.	Mixed phase	40	Grains		91	[36]
Ali et al.	Mixed phase	10.30	Grains	2.77		[37]

films due to the large value of crystallite size, less defects and a decrease of grain boundary area compared to high Zn doped CdO films which are confirmed by XRD results. The good conductivity observed in the films suggests that CdZnO with high Cd content film is a potential candidate for applications such as photodiodes, phototransistors, photovoltaic cells, transparent electrodes, liquid crystal displays, optical limiter and optical switching. Table 5 indicates the comparison of 50% Zn doped CdO film with previously published reports.

4 Conclusion

TCO of Cd_{1-x}Zn_xO films were grown on a glass substrate at different substrate temperatures using 0.05M molarity of Cadmium acetate and Zinc acetate solution through spray pyrolysis technique. The deposition temperature was optimized for different composition films to get uniform, homogeneous, stoichiometry and highly adherent films. All deposited films were polycrystalline in nature. The films of $x < 60\%$ and $x = 90\%$ of Zn content shown the single phase of cubic and hexagonal phases having (1 1 1) and (1 0 1) prominent planes respectively. The films of 50–80% Zn composition has shown a mixture of hexagonal-cubic phases. A gradual change of crystallite size, dislocation density and strain was noticed with increasing Zn content except for 70%. The uniform spherical grain observed for all deposits except 90% Zn composition in the film which shown fiber structure. The enhancement of optical transmittance and blue shift of absorption edge was found with increasing deposition temperature, and Zn content indicates the widening of the optical energy band gap. Optical parameters like optical conductivity, extinction coefficient, and Urbach energy were shown a systematic variation in deposition temperature and Zn content in the deposited films. All deposits shown n-type semiconductor nature. Enhancement of electrical resistivity with Zn content in the deposited films is mainly due to the reduction of carrier concentration and crystallite sizes. It is

concluded that the tuning of the optical band gap and resistivity of deposit films with varying deposition temperature and Zn concentration is helpful to be used as a potential candidate for the optoelectronic device.

Acknowledgements One of the authors (SJ) would like to thank Manipal University for granting junior research fellowship and providing experimental facilities. The authors thank UGC-DAE Consortium for Scientific Research, Mumbai Center India for sanctioning research projects (UDCSR/MUM/AO/CRS-M-212/2015/511).

References

1. L. Beaur, T. Bretagnon, T. Guillet, C. Brimont, M. Gallart, B. Gil, P. Gilliot, C. Morhain, Phonon-assisted exciton formation in ZnO/(Zn,Mg) O singlequantum wells grown on C-plane oriented substrates. *J. Lumin.* **136**, 355–357 (2013)
2. J. Santos-Cruz, G. Torres-Delgado, R. Castanedo-Perez, S. Jimenez-Sandoval, J. Marquez-Marin, O. Zelaya-Angel, Influence of the growth parameters of p-CdTe thin films on the performance of Au-Cu/pCdTe/n-CdO type solar cells. *Solar Energy* **80**, 142–147 (2006)
3. Y.D. Liu, J.S. Lian, Optical and electrical properties of aluminum-doped ZnO thin films grown by pulsed laser deposition. *Appl. Surf. Sci.* **253**, 3727–3730 (2007)
4. M. Li, J. Xu, X. Chen, X. Zhang, Y. Wu, P. Li, X. Niu, C. Luo, L. Li, Structural and optical properties of cobalt doped ZnO nanocrystals. *Superlattices Microstruct.* **52**, 824–833 (2012)
5. O. Alvarez-Fregozo, J.C. Mendoza-Alvarez, F. Sanchez-Sinocio, A. Huanosta, The growth and structure of Cd_{0.95}Fe_{0.05}Te thin films grown by radiofrequency sputtering. *J. Appl. Phys.* **64**, 3928–3933 (1988)
6. U. Ozgur, Y.I. Alivov, C. Liu, A. Teke, M.A. Reshchikov, S. Dogan, V. Avrutin, S.J. Cho, H. Morkoc, A comprehensive review of ZnO materials and devices. *J. Appl. Phys.* **98**, 103 (2005)
7. K.S. Hwang, Y.J. Lee, S. Hwangbo, Growth, structure and optical properties of amorphous or nano-crystalline ZnO thin films prepared by pre-firing-final annealing. *J. Ceram. Process. Res.* **8**, 305–311 (2007)
8. X.M. Zhang, M.Y. Lu, Y. Zhang, L.J. Chen, Z.L. Wang, Fabrication of a high-brightness blue-light-emitting diode using a ZnO-nanowire array grown on p-GaN thin film. *Adv. Mater.* **21**, 2767–2770 (2009)

9. S.-E. Ahn, H.J. Ji, K. Kim, G.T. Kim, C.H. Bae, S.M. Park, Y.-K. Kim, J. S. Ha, Origin of the slow photoresponse in an individual sol-gel synthesized ZnO nanowire. *Appl. Phys. Lett.* **90**, 153106–153109 (2007)
10. K.L. Chopra, S. Ranyan, Das, *Thin Film Solar Cells* (Plenum Press, New York, 1993)
11. A. Srivastava, R.K. Shukla, K.P. Misra, Photoluminescence from screen printed ZnO based nanocrystalline films. *Cryst. Res. Technol.* **46**, 949–955 (2011)
12. S. Vijayalakshmi, S. Venkataraj, R. Jayavel, Characterization of cadmium doped zinc oxide (Cd: ZnO) thin films prepared by spray pyrolysis method. *J. Phys. D* **41**, 245403–245410 (2008)
13. G.M. Li, X.C. Wang, Y.H. Wang, X.W. Shi, N. Yao, B.L. Zhang, Synthesis and field emission properties of ZnCdO hollow micro-nano spheres. *Physica E* **40**, 2649–2653 (2008)
14. S. Sadofev, S. Blumstengel, J. Cui, J. Puls, S. Rogaschewski, P. Schafer, F. Henneberge, Visible band-gap ZnCdO heterostructures grown by molecular beam epitaxy. *Appl. Phys. Lett.* **89**, 201907–201910 (2006)
15. R. Vettumperumal, S. Kalyanaraman, B. Santoshkumar, R. Thangavel, Magnetic properties of high Li doped ZnO sol gel thin films. *Mater. Res. Bull.* **50**, 7–11 (2013)
16. G. Ferblantier, A. Boyer, A. Foucaran, Electrical properties of zinc oxide sputtered thin films. *Microelectron. J.* **34**, 1087–1092 (2003)
17. F. Osvaldo Vigil, G. Cruz, G. Santana, Contreras-Puente, Influence of post-thermal annealing on the properties of sprayed cadmium–zinc oxide thin films. *Appl. Surf. Sci.* **161**, 27–34 (2000)
18. R.K. Gupta, M. Cavas, F. Yakuphanoglu, Structural and optical properties of nanostructure CdZnO films. *Spectrochim. Acta Part A* **95**, 107–113 (2012)
19. A.M. Guillermo Santana, O. Acevedo, Vigil, Structural and optical properties of $(\text{ZnO})_x(\text{CdO})_{1-x}$ thin films obtained by spray pyrolysis. *Thin Solid Films* **373**, 235–238 (2000)
20. Y.R. Sui, Y.P. Song, Y.G. Yue, B. Yao, Y. Cao, J.H. Lang, X.Y. Li, J.H. Yang, Cd composition induced effects on structure, optical and electrical properties of sputtered $\text{Zn}_{1-x}\text{Cd}_x\text{O}$ films. *Ceram. Int.* **41**, 5414–5420 (2015)
21. I. Singh, R.K. Bedi, Studies and correlation among the structural, electrical and gas response properties of aerosol spray deposited self-assembled nanocrystalline CuO. *Appl. Surf. Sci.* **257**, 7592–7599 (2011)
22. K. Usharani, A.R. Balu, Structural, optical and electrical properties of Zn-Doped CdO thin films fabricated by a simplified spray pyrolysis technique. *Acta Metall. Sin. (Engl. Lett.)* **28**(1), 64–71 (2015)
23. M. Azizar Rahman, M.K.R. Khan, Effect of annealing temperature on structural, electrical and optical properties of spray pyrolytic nano crystalline CdO thinfilms. *Mater. Sci. Semicond. Proc.* **24**, 26–33 (2014)
24. Z. Ye, D. Ma, J. He, J. Huang, B. Zhao, X. Luo, Z. Xu, Structural and photoluminescent properties of ternary $\text{Zn}_{1-x}\text{Cd}_x\text{O}$ crystal films grown on Si(1 1 1) substrates. *J. Cryst. Growth* **256**, 78–82 (2003)
25. V. Khranovskyy, A. Ulyashin, G. Lashkarev, B.G. Svensson, R. Yakimova, Morphology, electrical and optical properties of undoped ZnO layers deposited on silicon substrates by PEMOCVD. *Thin Solid Films* **516**, 1140–1396 (2008)
26. B.E. Sernelius, K.F. Berggren, Z.C. Jin, I. Hamberg, C.G. Granqvist, Band-gap tailoring of ZnO by means of heavy Al doping. *Phys. Rev. B* **37**, 10244–10248 (1988)
27. T.K. Subramanyam, B. Srinivasulu Naidu, S. Uthanna, Studies on dc magnetron sputtered cadmium oxide films. *Appl. Surf. Sci.* **169**, 529–534 (2001)
28. S.S. Shinde, P.S. Shinde, Y.W. Oh, D. Haranath, C.H. Bhosale, K.Y. Rajpure, Structural, optoelectronic, luminescence and thermal properties of Ga-doped zinc oxide thin films. *Appl. Surf. Sci.* **258**, 9969–9976 (2012)
29. H. Tabet-Derrazn, N. Benramdane, D. Nacer, A. Bouzidi, M. Medles, Investigations on $\text{Zn}_x\text{Cd}_{1-x}\text{O}$ thin films obtained by spray pyrolysis. *Sol. Energy Mater. Sol. Cells.* **73**, 249–259 (2002)
30. M.S. Gowrishankar, L. Balakrishnan, N. Gopalakrishnan, Band gap engineering in $\text{Zn}_{(1-x)}\text{Cd}_x\text{O}$ and $\text{Zn}_{(1-x)}\text{Mg}_x\text{O}$ thin films by RF sputtering. *Ceram. Int.* **40**, 2135–2142 (2014)
31. X. Tang, H.F. Lu, J.J. Zhao, Q.Y. Zhang, Study on the doping stability and electronic structure of wurtzite $\text{Zn}_{1-x}\text{Cd}_x\text{O}$ alloys by first-principle calculations. *J. Phys. Chem. Solids* **71**, 336–339 (2010)
32. P.K. Ghosh, S. Das, S. Kundoo, K.K. Chattopadhyay, Effect of fluorine doping on semiconductor to metal-like transition and optical properties of cadmium oxide thin films deposited by sol-gel process. *J. Sol-Gel Sci. Technol.* **34**, 173–179 (2005)
33. H. Czichos, T. Saito, L. Smith. *Handbook of Materials Measurement Methods*, vol. 978 (Springer, Leipzig, 2006)
34. S.H. Chaki, M.P. Deshpande, J.P. Taylor, Characterization of CuS nanocrystalline thin films synthesized by chemical bath deposition and dip coating techniques. *Thin Solid Films* **550**, 291–297 (2014)
35. M. Ohyama, H. Kozuka, T. Yoko, Sol-gel preparation of transparent and conductive aluminum-doped zinc oxide films with highly preferential crystal orientation. *J. Am. Ceram. Soc.* **81**, 1622–1632 (1998)
36. Y. Caglar, M. Caglar, S. Ilcan, A. Ates, Morphological, optical and electrical properties of CdZnO films prepared by sol-gel method. *J. Phys. D* **42**, 065421–065428 (2009)
37. M. Ali Yıldırım, Sümeyra Tuna Yıldırım, Aytunç Ateş, Cadmium concentration effect on structural, optical and electrical properties of nanostructured $\text{Cd}_x\text{Zn}_{1-x}\text{O}$ thin films. *J. Alloys Compd.* **17**, 30112–30113 (2017)